

## The removal of Ni & Cu from a mixed metal system using sodium borohydride as a reducing agent

N.T Sithole, F. Ntuli<sup>1</sup>, T. Falayi

*University of Johannesburg, Department of Chemical Engineering, School of Mining, Metallurgy and Chemical Engineering, P.O. Box 17011, Doornfontein 2088, South Africa*

### Abstract

---

Removal of nickel (II) and copper (II) from aqueous solutions using NaBH<sub>4</sub> as a reducing agent was studied. Reduction crystallization was achieved in a batch reactor at 65°C using seeded experiments. The effect of using different molar ratios of [Ni<sup>2+</sup>]:[BH<sub>4</sub><sup>-</sup>] namely; 1:1, 1:0.25 and 1:0.1 and seeding materials on the rate of reduction was also investigated. The results obtained showed that NaBH<sub>4</sub> is an effective reducing agent for the removal of Ni<sup>2+</sup> and Cu<sup>2+</sup> from effluents. Using a molar ratio of 1:0.1 of [Ni<sup>2+</sup>]:[BH<sub>4</sub><sup>-</sup>] and Fe and Ni as a seeding material over 99% metal removal was achieved. Ni as a seeding material yielded the best results as it is autocatalytic although there was no significant difference in the rate of reduction compared to that obtained when Fe was used as a seeding material.

**Key words:** *reduction crystallization, precipitation kinetics, heavy metal removal, sodium borohydride*

---

<sup>1</sup>Email: [fntuli@uj.ac.za](mailto:fntuli@uj.ac.za) tel: +27115596003, Fax: +27 11 559 6430

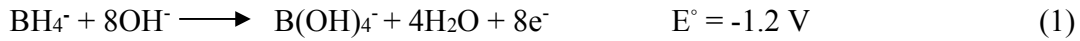
## INTRODUCTION

The presence of base metals in water resources is a worldwide environmental problem and poses disposal problems due to their non-biodegradability and persistence in the environment (Audullah, 2009). Copper and nickel are toxic metals which may be accumulated in the human or ecological food chain through consumption or uptake and may be hazardous to human health or the environment. Drinking water which has higher level of metals in it may cause vomiting, diarrhea and stomach cramp (Tasker, 2007).

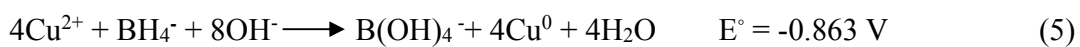
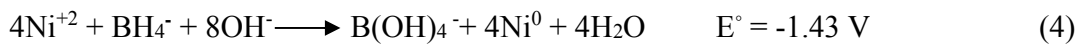
Wastewater is discharged from a number of industries such as mining and metal refineries. Several techniques such as chemical precipitation, electrolytic membranes and ion exchange are used for removal of metals ions from aqueous solution. These methods are efficient but they are not widely used due to high cost, low feasibility for small scale and regeneration of the material (Bulut *et al.*2007; Hazar, 2003). Precipitation is the mostly widely used wastewater treatment method, because it is the most economical method and easier to implement and operate on a large scale. However, traditional precipitation methods using lime, sulphides or hydroxides recover metals in the form of a voluminous sludge which is not reusable and has to be disposed in landfills creating a potential environmental hazard, loss of valuable mineral and further treatment is required with high operational costs particularly, high energy consumption (Phetla *et al.*2012) .

As the natural sources for metals are dwindling, it is becoming more economical to recover heavy metals in their metallic state and reuse the metals obtained. A modified precipitation process, reduction crystallization, which allows heavy metal to be removed and recovered in their elemental state as metallic powders by using reducing agent was explored (Naboychenko, 2009). Reducing agents such as sodium hypophosphite, hydrazine and formaldehyde have been used in a variety of chemical reactions from organic compounds synthesis to metal production (Mallory, 1990). Previous studies using nickel powder as seeding material have demonstrated that hydrazine and sodium hypophosphite are effective reducing agents for Ni, Cu, Co and Fe with removal efficiencies of over 97% and 80% respectively (Phetla *et al.* 2012; Horikwa *et al.* 2000). Based on these findings the feasibility of using the same technique with a different

reducing agent, sodium borohydride, was explored. The principal half reaction of the borohydride ion with Ni and Cu are given in equations 1-5:



Equation 1 shows the principal half reaction occurring when the borohydride ion is used as a reducing agent. Combining equation 1, 2 and 3 gives the overall reactions that are:



From equations 4 and 5 it is shown that the  $\text{BH}_4^-$  ion can theoretically reduce four moles of  $\text{Ni}^{2+}$  and  $\text{Cu}^{2+}$  respectively, indicating a preferred  $[\text{M}^{2+}]:[\text{BH}_4^-]$  molar ratio of 1:0.25. However, previous experimental studies suggest that one mole of borohydride reduces approximately one mole of nickel indicating a preferred  $[\text{M}^{2+}]:[\text{BH}_4^-]$  molar ratio of 1:1 (Mallory, 1990). Thus there is a need to establish the effect of the molar ratio of  $[\text{M}^{2+}]:[\text{BH}_4^-]$  on the reduction crystallization behavior of metals from solution. In this study molar ratios of  $[\text{M}^{2+}]:[\text{BH}_4^-]$  above and below the stoichiometric amounts as established by equations 4 and 5 were investigated.

Previous studies (Phetla *et al.*, 2012; Naboycheko, 2007; Horikwa *et al.*, 2000) showed that using nickel powder as a seeding material in reduction crystallization, increases the effective catalytic surface area of Ni seed until the total area is uniformly active hence accelerating the rate of reduction. However, the use of other catalytic powders such as iron and copper as seeding materials in reduction crystallization has not been well studied. Based on this fact the feasibility of using a cheaper seeding material (Fe) was explored.

## MATERIALS AND METHODS

### *Experimental apparatus*

A 2 L batch reactor fitted with an overhead stirrer was used to ensure adequate suspension of the seeding material in solution. A thermometer was used to measure

temperature. A potentiometer-pH meter was used to measure the pH and potential during the reduction crystallization process. A heating mantle was used to heat the solution to speed up the reaction. Atomic absorption spectroscopy (AAS; Tescan Vega 3 XMU I) was used to measure the concentrations of Ni and Cu in solution after reduction. A Malvern particle size analyser, Mastersizer (2000) was used to measure the particle size distribution (PSD) of the powder using a laser diffraction technique. The powder morphology was captured using a scanning electron microscopy (SEM; Thermo scientific ICE 3000 series). Fourier transform infrared spectroscopy (Thermoscientific Nicolet IS10) was used to characterize the seeding material powder before and after the reduction crystallization experiments.

### ***Materials***

CuSO<sub>4</sub>·5H<sub>2</sub>O and NiSO<sub>4</sub>·6H<sub>2</sub>O salts supplied by Sigma Aldrich were used to prepare the synthetic 0.5 g/l Cu<sup>2+</sup> solution and Ni<sup>2+</sup> solution. Ni and Fe powder supplied by Sigma Aldrich were used as seeding materials. Reverse osmosis water was used to prepare all the solutions. NaOH supplied by Rochelle chemicals was used to adjust the pH. HNO<sub>3</sub> and H<sub>2</sub>SO<sub>4</sub> were supplied by Sigma Aldrich and were used for sample digestion in preparation for AAS analysis.

### ***Preparation of solutions***

3.36 g of NiSO<sub>4</sub>·6H<sub>2</sub>O was added to 500 ml of Reverse Osmosis (RO) water. The solution was agitated until the salt was dissolved. The resulting solution was then made up to 1500 ml to make a 0.5 g/L Ni<sup>2+</sup>. The above procedure was also used to prepare 0.5 g/L of Cu<sup>2+</sup> by using 2.95 g of CuSO<sub>4</sub>·5H<sub>2</sub>O. For the mixed solution 3.36 g of NiSO<sub>4</sub>·6H<sub>2</sub>O and 2.95 g of CuSO<sub>4</sub>·5H<sub>2</sub>O were used to make up a 0.5 g/L of Ni<sup>2+</sup> and Cu<sup>2+</sup> respectively.

### ***Experimental procedure***

500 ml of 0.5 g/l of Ni<sup>2+</sup> was mixed with 0.32 g of NaBH<sub>4</sub> and a predetermined amount of the seeding material (powder) in a 2 L batch reactor. The solution represented a 1:1 molar ratio of [Ni<sup>2+</sup>]:[BH<sub>4</sub><sup>-</sup>]. The resulting solution was then heated to 65°C and then the pH was adjusted to 12 by adding 70 ml of 1 M NaOH. The reduction crystallization

reaction was allowed to occur for 3 min during which the pH and electrode potential were measured after every 30 s. Thereafter, agitation and heating was stopped and the solution was allowed to cool. After settling, the clear supernatant was decanted carefully leaving the seeding material and reduced metal in the reactor. The above procedure was repeated twice with fresh Ni solution and the same seeding material. After the third batch reduction the seeding material was discharged from the reactor. The seeding material was filtered and washed using a Buchner vacuum filtration unit and air dried for particle size distribution and morphology analysis. The reduced solution was then filtered and 100 ml of the sample was analysed for the residual metal concentration using AAS. To study the effect of the  $[\text{Ni}^{2+}]:[\text{BH}_4^-]$  molar ratio a similar procedure was repeated where 0.0806 g and 0.032 g of  $\text{NaBH}_4$  was used to prepare solutions with molar ratios of 1:0.25 and 1:0.1 respectively. A similar procedure was also used to investigate the effect of different seeding materials where a mixed solution of Cu and Ni containing 0.5 g/L  $\text{Ni}^{2+}$  and 0.5 g/L  $\text{Cu}^{2+}$  was used. 30 g of each seeding material was used in these experiments. The above experiments were repeated with a variation in the solid loading of the seeding material without the adjustment of pH.

### ***Sample analysis***

The concentration of Ni and Cu in the reduction solutions was analysed using AAS. 2 ml of 1:1  $\text{HNO}_3$  and 1 ml of 1:1  $\text{HCl}$  were added into 100 ml of filtered reduced solution. Volume reduction to 20 ml was achieved by heating the solution to  $80^\circ\text{C}$ . Then the sample was poured in a 50 ml conical flask and made up to volume with RO water. The sample was ready for AAS analysis. The above procedure was used to prepare all the AAS samples for analysis.

The powder (seeding material and metallic powder produced by reduction) was carbon coated for SEM analysis. To determine the purity of the powder, 5 g of powder (seeding material and metallic powder produced) was pressed into a pellet for XRF analysis. 0.1 g of the seeding material was used for FTIR analysis.

### ***Statistical analysis of data***

Each run was done in duplicates with results within 5% of each other being averaged. A single factor ANOVA was used to compare the significant difference in the reduction of

metal between different molar ratios of  $[M^{2+}]:[BH_4^-]$ . Furthermore a student  $t$  test with the assumption of unequal variance was used to compare significance of the difference in metal reduction between Ni and Fe seeding material.

## RESULTS AND DISCUSSION

### Effect of solid loading without pH adjustment

Figure 1 shows the variation of  $Ni^{2+}$  and  $Cu^{2+}$  % removal without the addition of NaOH at three batch densification each using Ni powder as a seeding material at different solid loading with  $NaBH_4$  as a reducing agent.

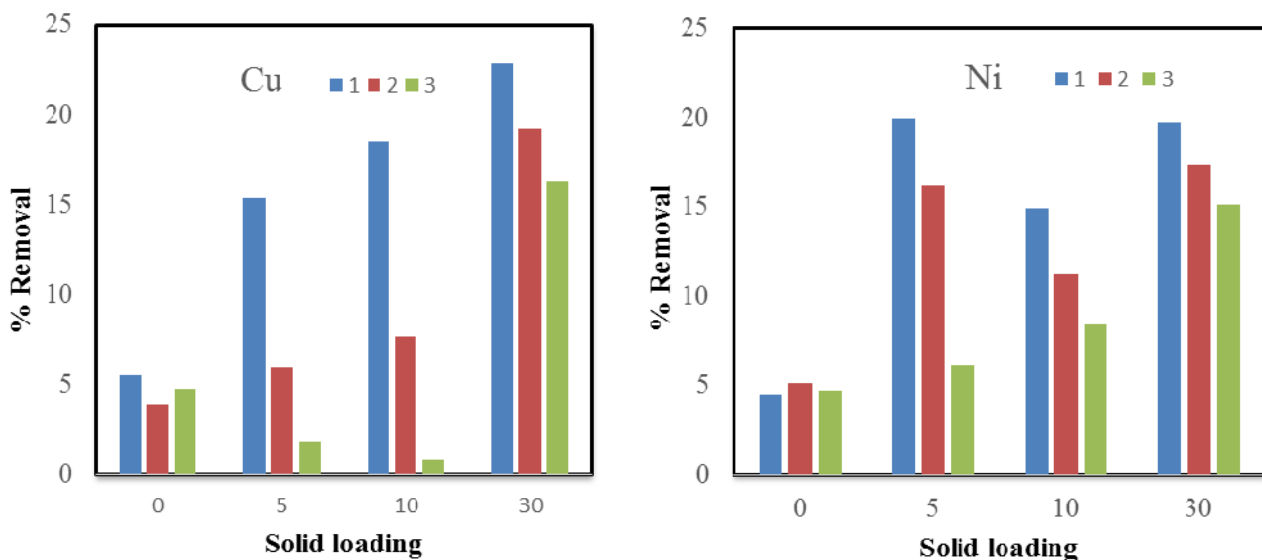


**Fig 1: Variation of Ni and Cu % removal at different solid loading**

Fig 1 shows that Cu and Ni % removal increases with an increase in solid loading and decreases as the seed is reused. At 0% solid loading (no seeding material added), the lowest % removal was obtained compared to the reduction performed with a seeding material. There was no significant difference in pH from the 1<sup>st</sup> to the 3<sup>rd</sup> densification which ranged between 6.8 and 7.2. Therefore, for reduction crystallization to take place seeding material loading and pH adjustment are critical as reported by Horikwa, 2000 and Mallory, 1990 Therefore the solid loading of 30 g and pH adjustment using NaOH was used for subsequent experiments in line with previous reduction crystallization

experiment (Phetla *et al* ,2012; Horikawa, 2000; Malematja, 2012; Jianming *et al.* 1997; Naboychenko, 2009).

### ***Effect of $BH_4^-$ concentration***

The removal efficiency was calculated using equation 6 below

$$\text{Removal efficiency} = \frac{[Ni]_{initial} - [Ni]_{final}}{[Ni]_{initial}} \times 100 \% \quad (6)$$

Figure 2 shows the variation in the metal removal with different  $[Ni^{2+}]:[BH_4^-]$  molar ratios using Ni as seeding material.

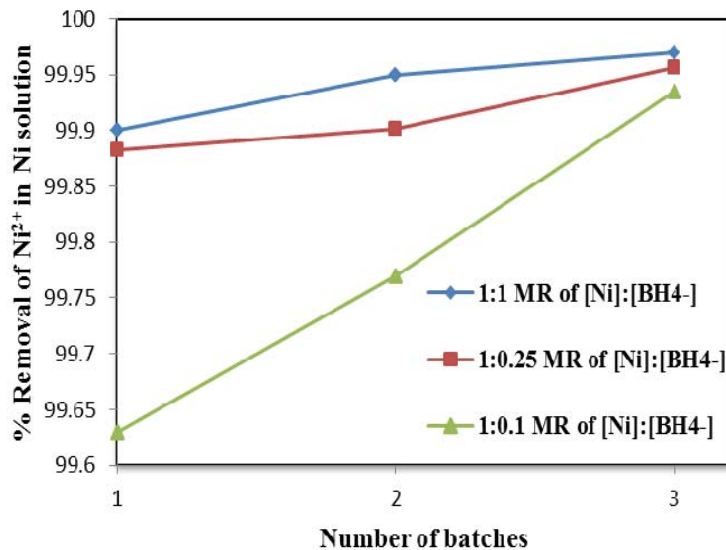


**Fig. 2: % removal of  $Ni^{2+}$  using Ni as seeding material at different  $[Ni^{2+}]:[BH_4^-]$  molar ratios**

The highest %Ni removal of 99.96% was achieved using a 1:1 molar ratio of  $[Ni^{2+}]:[BH_4^-]$ , while the lowest %removal was 99.63% using 1:0.1 molar ratio. Increasing the molar ratio above the stoichiometric amount of 1:0.25 increased the % Ni removal while decreasing it decreases the % Ni removal. The reduction of Ni increased with each batch reduction, due to plating of Ni which has an autocatalytic effect that increases removal efficiency. A single factor Anova was used to compare the difference in % Ni removal at  $[Ni^{2+}]:[BH_4^-]$  molar ratios of 1:0.1, 1:0.25 and 1:1. A *p* value of 0.142 was

obtained against a critical  $P$  value of 5.14 at 95% confidence interval. This therefore means there is no significant difference between the % Ni removal at 1:0.1, 1:0.25 and 1:1 molar ratios of  $[\text{Ni}^{2+}]:[\text{BH}_4^-]$ . Based on this finding a 1:0.1 molar ratio was chosen for all other experiments, since it is more economical to use lower concentrations of the reducing agent. This also reduces the amount of impurities incorporated into the powder as a result of the oxidation of the borohydride ion and the concentration of B in the residual solution.

***Evolution of the pH and potential during reduction***

The evolution of the pH and potential with respect to the SHE at different molar ratios of  $[\text{Ni}^{2+}]: [\text{BH}_4^-]$  is shown in Table 1.

**Table 1: Evolution of the pH–redox potential at different  $[\text{Ni}^{2+}]:[\text{BH}_4^-]$  molar ratios with each experiment repeated.**

time (s)	1 <sup>st</sup> run, 1:1		2 <sup>nd</sup> run, 1:1		1 <sup>st</sup> run, 1:0.25		2 <sup>nd</sup> run, 1:0.25	
	pH	mV	pH	mV	pH	mV	pH	mV
30	11.89	-312.5	12.05	-315.0	12.35	-315.0	11.96	-305.0
60	11.91	-315.0	12.08	-315.0	12.05	-312.0	11.96	-305.5
90	11.92	-317.0	12.10	-316.0	12.3	-317.5	11.98	-306.0
120	11.92	-319.5	12.10	-321.5	12.33	-318.0	12.00	-306.5
150	11.90	-320.0	12.10	-314.5	12.46	-320.0	11.96	-306.5
180	11.94	-320.5	12.09	-312.0	12.5	-307.5	11.94	-307.0

time (s)	1 <sup>st</sup> run, 1:0.1		2 <sup>nd</sup> run, 1:0.1	
	pH	mV	pH	mV
30	12.30	-304.5	12.25	-303.5
60	12.28	-305.0	12.24	-304.5
90	12.27	-305.5	12.23	-304.5
120	12.26	-305.5	12.22	-304.5
150	12.26	-306.5	12.22	-304.5
180	12.26	-306.5	12.22	-304.5



Both the reduction potential and the pH decreased as the reaction proceeded. This is expected since the reduction of nickel generates  $H^+$  ions. The reduction potential was more negative at a  $[Ni^{2+}]:[BH_4^-]$  molar ratio of 1:1 and decreased with decrease in the  $[Ni^{2+}]:[BH_4^-]$  molar ratio, indicating that the reduction rate is strongly affected by the concentration of the  $BH_4^-$  ion in solution.

#### *Effect of reduction crystallization on particle morphology*

Fig.3 shows the micrographs of the nickel seeding material and nickel powder after reduction crystallization respectively. The morphology at all molar ratios were the same hence only one micrograph is shown for samples after reduction crystallization.

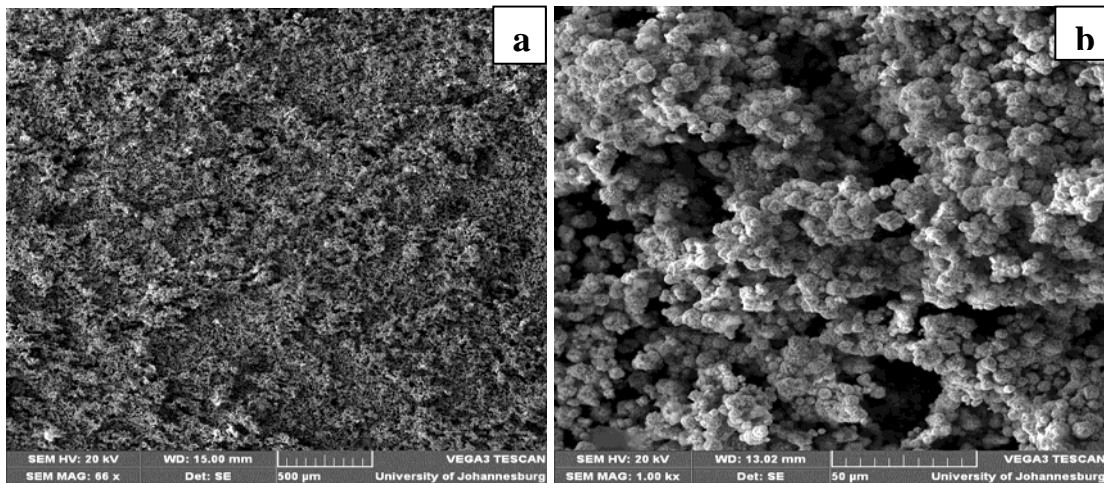


**Fig. 3: (a) SEM micrograph of Nickel seed before reduction, (b) SEM micrograph of powder produced at at  $[Ni^{2+}]: [BH_4^-]$  molar ratio of 1:1**

Fig. 3 (b) shows that there was a change in the morphology of the particles from that of the seed in Fig 3(a). The particles appeared flaky and fluffy and closely packed before reduction crystallization but after reduction process, they were spherical and porous.

#### *Nickel powder purity*

Table 2 shows the XRF analysis of the seeding material before and after reduction.

**Table 2: Elemental compositions of powders produced at different [Ni<sup>2+</sup>]:[BH<sub>4</sub><sup>-</sup>] molar ratios**

Elements	Before reduction	After reduction		
	Ni Seed	1:1	1:0.25	1:0.1
Na	0.000	0.565	0.873	0.982
Al	0.0551	0.215	0.233	0.186
Si	0.0830	0.334	0.373	0.298
S	0.0130	0.074	0.124	0.147
Fe	0.0401	0.0202	0.0109	0.0101
Ni	99.8	98.7	98.3	98.1

The elemental composition can be directly related to the powder purity and it can be noted from Table 2 that the Ni content decreased with a decrease in NaBH<sub>4</sub> concentration. This indicates that the amount of Ni plated increases with increase in the [Ni<sup>2+</sup>]:[BH<sub>4</sub><sup>-</sup>] molar ratio. The nickel content decreased as a result of incorporation of impurities generated as a result of the decomposition of NaBH<sub>4</sub> on the Ni seed with Na being the major impurity. However, boron was not detected in the Ni powder as noted in previous studies (Mallory, 1990; Jianming *et al.*1997). **The decrease in the relative proportion of Fe in the seed indicates that it participates in the cementation reaction to a greater extent than Al (Table 2). The proportion of Fe also decreases with decrease in Ni:BH<sub>4</sub><sup>-</sup> molar ratios, indicating that the extent of cementation increases with decrease in molar ratio. The factor above explains why reduction still occurs at molar ratios lower than the stoichiometric values. Displacement of Ni from solution by more electropositive metals like Fe (cementation) in the seeding material is illustrated by equation 7.**



### Evolution of the PSD

Fig. 4 (a) shows the volume distribution of the powder and (b) shows the evolution of the number distribution of the powder produced using different molar ratios of  $[\text{Ni}^{2+}]:[\text{BH}_4^-]$ .

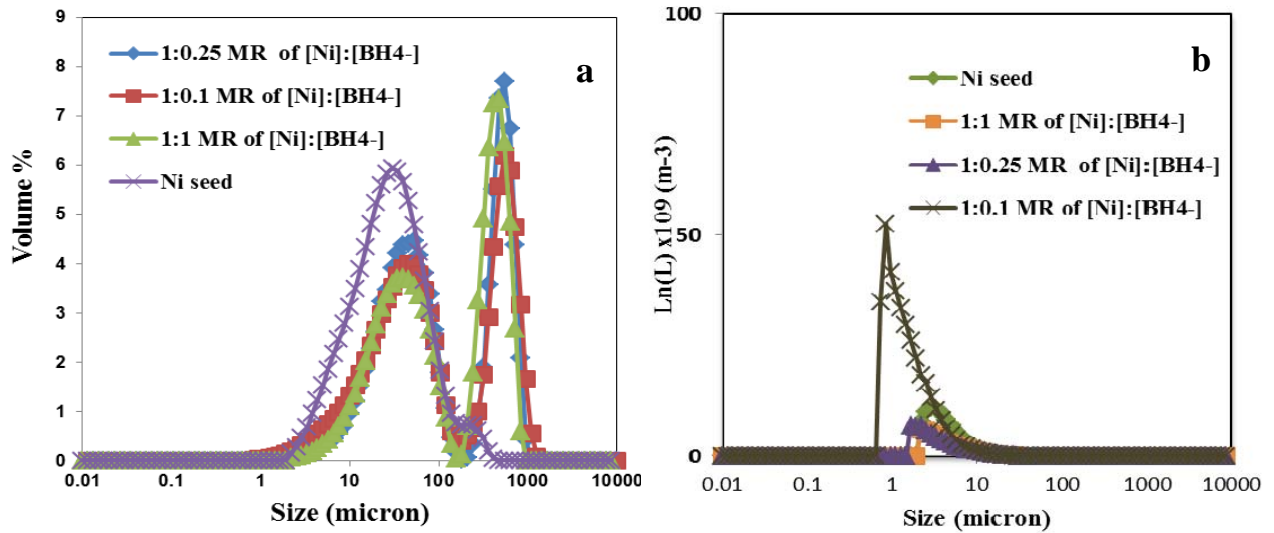


**Fig. 4: (a) Evolution of PSD by volume and (b) Evolution of PSD by number distribution**

There was a significant change in the volume distribution of the powder produced at all molar ratios from a uni-modal to a bimodal distribution relative to the Ni seed. The bi-modal distribution is typical of aggregation/agglomeration during particle formation, indicating that agglomeration may have occurred during reduction. This finding is also confirmed by SEM micrographs of the powder produced (Fig. 4a). Due to either particle growth/agglomeration there was an increase in volume of the particles with a size greater than 100  $\mu\text{m}$  with a corresponding reduction in the volume of particles of less than 100  $\mu\text{m}$ . Fig 4(b) shows that reduction crystallization resulted in a significant increase in the number of smaller sized particles for 1:0.1 molar ratio of  $[\text{Ni}^{2+}]:[\text{BH}_4^-]$ , which is likely to be due to nucleation. Furthermore there was a shift in the PSD to the left from that of the seed indicating the generation of fines. There was also a decrease in the area under the curve at molar ratios of 1:0.25 and 1:1 indicating a decrease in particle number, evidence of aggregation.

### ***Moments of the PSD and Crystallization kinetics***

The PSD data was transformed into its moments using equations 8 and 9. The number density function was calculated from the volume based histogram vol% versus  $L_i$  where  $i$  indicates the size sub-range and the particle concentration (vol %) were generated by laser diffraction and the volume shape factor  $k_v$  equal to  $\pi/6$  was used

$$n(L)dL = \frac{\sum \text{vol}\% \times \text{conc}(\text{vol}\%)}{100} \times \frac{1}{k_v L^3} \quad (8)$$

The moments of the PSD were calculated from the number density function  $[n(L)]$  with respect to internal coordinate  $L$ , using equation 8:

$$m_i = \int_0^{\infty} L^i n(L) dL \quad (9)$$

The external surface area and number of particles was calculated using the method of moments to calculate the zeroth ( $m_0$ -equivalent to particle number) and the second moment ( $m_2$ -equivalent to external surface area) and the results are shown in Table 3.

**Table 3: Moments of Ni powder before and after reduction**

	<b>Before reduction</b>	<b>molar ratio of <math>[\text{Ni}^{2+}]:[\text{BH}_4^-]</math></b>		
	Ni seed	1:1	1:0.25	1:0.1
Particle number ( $\# \cdot \text{m}^{-3} \times 10^{13}$ )	8.61	4.45	5.87	37.1
External surface area ( $\text{m}^2 \cdot \text{m}^{-3} \times 10^3$ )	3.80	3.09	3.09	3.79

There was an overall decrease in particle number and external surface area as compared to the seeding material at  $[\text{Ni}^{2+}]:[\text{BH}_4^-]$  molar ratios of 1:1 and 1:0.25 due to particle aggregation. At a molar ratio of 1:0.25, there an increase in particle number relative to seeding material and a decrease in external surface area, possibly due to nucleation and aggregation. Overall, there was an increase in both particle number and external surface

area with decrease in  $[\text{Ni}^{2+}]:[\text{BH}_4^-]$  molar ratio indicating the powder becomes less aggregated with decrease in the  $\text{BH}_4^-$  ion concentration.

Using the moments form of the population balance and assuming no breakage and size independent growth and aggregation, the molecular growth rate ( $G_0$ ), aggregation kernel ( $\beta$ ), aggregation rate ( $R_a$ ) and nucleation rate ( $B^0$ ) were calculated using equations 10-13 respectively (Hounslow *et al.*1988; Moussaoui *et al.*1997) and tabulated in Table 4.

$$G_0 = \frac{\Delta m_3}{3m_2\Delta t} \quad (10)$$

$$\beta = \frac{\Delta m_2}{(\overline{m_1})^2 \Delta t} - 2 \frac{G_0}{\overline{m_1}} \quad (11)$$

$$R_a = -\beta m_0^2 / 2 \quad (12)$$

$$B^0 = \frac{\Delta m_0}{\Delta t} + \frac{1}{2} \beta m_0^2 \quad (13)$$

**Table 4: Growth, nucleation and aggregation rates at different molar ratios of  $[\text{Ni}^{2+}]:[\text{BH}_4^-]$**

$[\text{Ni}^{2+}]:[\text{BH}_4^-]$ molar ratio	$G_0 \times 10^{-8}$ (m.s <sup>-1</sup> )	$B^0 \times 10^{11}$ (no/m <sup>3</sup> s)	$R_a \times 10^{11}$ (no/m <sup>3</sup> s)
1:1	3.49	-	8.47
1:0.25	2.71	-	6.57
1:0.1	1.57	2.21	1.93

The growth and aggregation rates all decreased significantly with the decreases in the  $[\text{Ni}^{2+}]:[\text{BH}_4^-]$  molar ratio. The nucleation rate was only positive at a molar ratio of 1:0.25. It is proposed that nucleation occurred at all molar ratios however; the rate of aggregation was much lower at molar ratios below the stoichiometric ratio leading to a less aggregated powder. Since nucleation is a function of supersaturation, and increases with increase in supersaturation it is likely that its effect at molar ratios of  $[\text{Ni}^{2+}]:[\text{BH}_4^-]$  higher than 1:0.1 was masked by the high aggregation rate. The shift of the modal size of the

number distribution to the left relative to that of the nickel seed (Fig. 5) indicates the production of smaller sized particles which are likely to be formed by nucleation.

***Metal removal from a mixed metal solution (Ni and Cu) using Ni as seeding material***

Figure 5 shows the variation of Ni<sup>2+</sup> and Cu<sup>2+</sup> % removal with the number of batches using Ni powder and a molar ratio of [Ni<sup>2+</sup>]:[BH<sub>4</sub><sup>-</sup>] and [Cu<sup>2+</sup>]:[BH<sub>4</sub><sup>-</sup>] of 1:0.1 respectively.

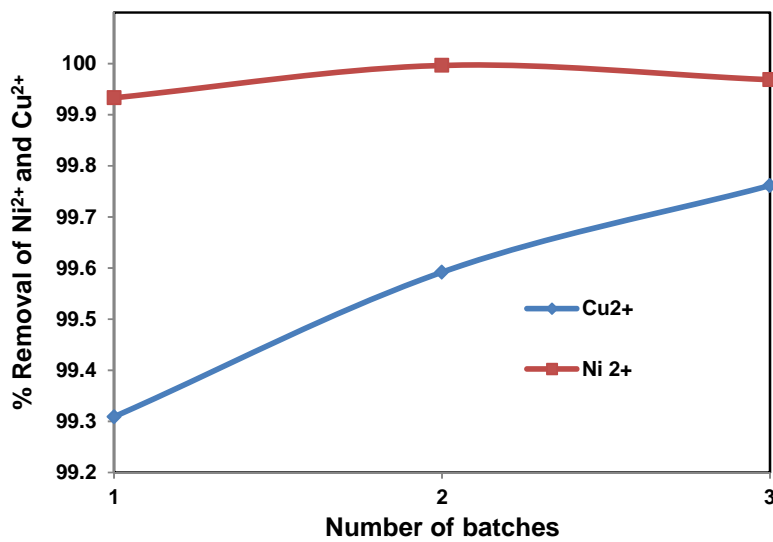


**Fig. 5: % Removal of Cu<sup>2+</sup> and Ni<sup>2+</sup> using Ni as a seed material**

Ni %removal of over 99.90% was achieved in all the three batch reductions as compared to Cu where %removal was below 99.76%. Ni was preferentially removed as compared to Cu<sup>2+</sup>. Since Ni is used as seed material it is proposed this favours the preferential deposition of Ni<sup>2+</sup> over Cu<sup>2+</sup> as also observed in previous studies (Phetla et al,2012 ). % removal of both Ni and Cu increased with each batch densification.

***Evolution of the PSD of the powder from a mixed metal solution***

A comparison of the PSD of the powder produced before and after reduction is shown in Fig. 6 using mixed metal solution (Ni<sup>2+</sup> and Cu<sup>2+</sup>) and Ni as seeding material.

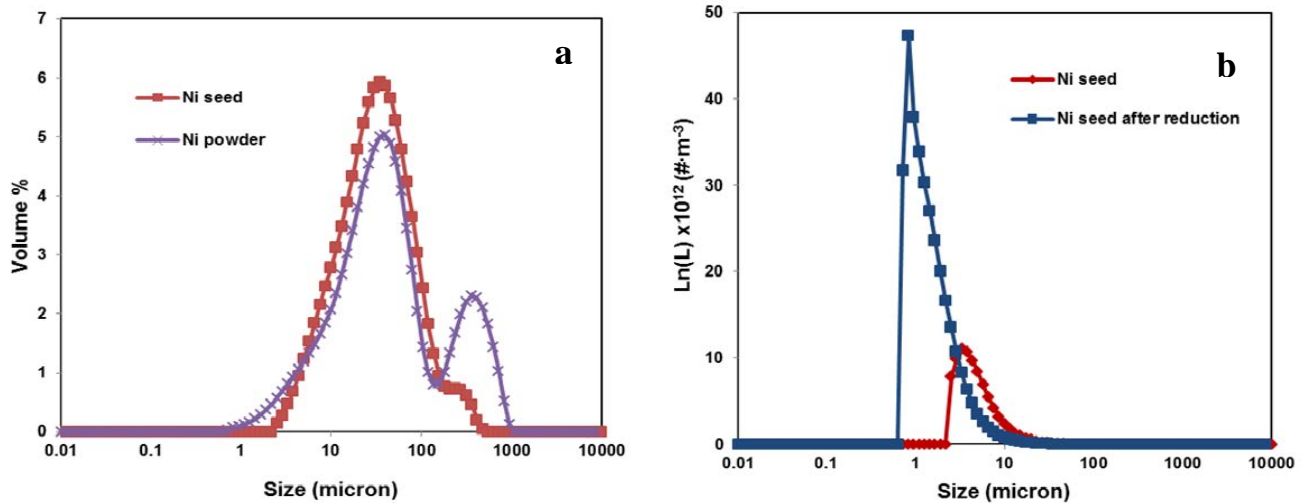


**Fig. 6 : (a) Evolution of PSD by volume and (b) evolution of PSD by number distribution using Ni powder as a seed**

The powder produced in fig 6(a) was characterized by a bimodal volume distribution after reduction crystallization. The bi-modal distribution is typical of aggregation/agglomeration during particle formation indicating agglomeration occurred during reduction crystallization. Fig 8(b) shows the number distribution of the nickel seed and powder produced after three batch reductions. There was a shift to the left relative to the Ni seed which indicate the generation of smaller sized particles by nucleation. The trends obtained are similar to those obtained from the Ni-only solution (Fig. 4).

***The effect of using Fe as seeding materials in a Mixed  $\text{Ni}^{2+}$  and  $\text{Cu}^{2+}$  solution***

Fig. 7 shows the variation of  $\text{Ni}^{2+}$  and  $\text{Cu}^{2+}$  % removal with the number of batches using Fe powder and a molar ratio of  $[\text{Ni}^{2+}]:[\text{BH}_4^-]$  and  $[\text{Cu}^{2+}]:[\text{BH}_4^-]$  of 1:0.1 respectively.

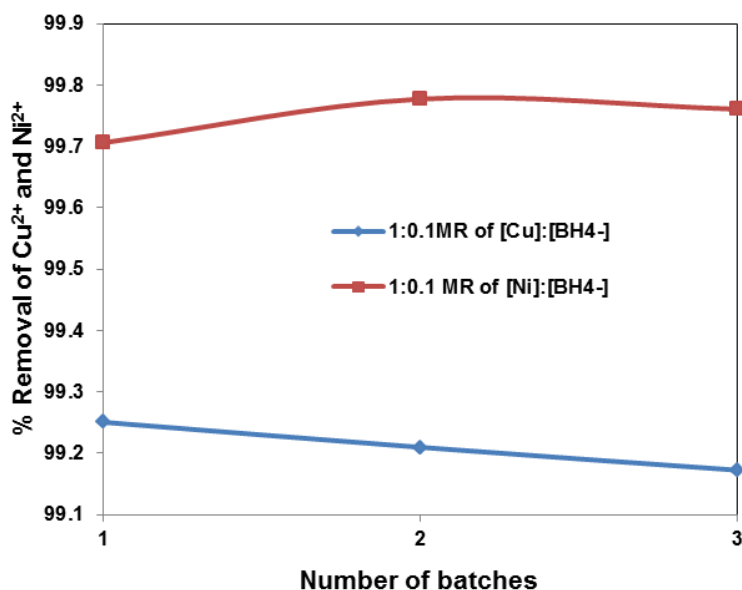


**Fig. 7: % Removal of Cu<sup>2+</sup> and Ni<sup>2+</sup> using Fe as seeding material**

Fig. 7 shows that the % removal of copper decreased from 99.26% to 99.17%, while that of Ni increased from 99.71% to 99.78% and thereafter decreased to 99.76%. The re-use of Fe seed decreased the % removals of Ni and Cu which implies, the seed was being passivated possibly by the incorporation of Cu which is less catalytically active compared to Ni. Based on the reduction potential of Ni (-0.23) and Cu (0.34), the reduction of Ni is thermodynamically more favorable than that of Cu. Hence, from the results obtained Ni is preferentially removed when compared to Cu. Since Fe is used as a seeding material it is proposed this favours the preferential deposition of Ni over Cu. Metals that are more electropositive than nickel e.g. Fe and Cu undergo a cementation reaction by displacing Ni from solution forming a nickel catalytic surface. Re- using the seed decreased the % removals of Cu to a large extent as compared to that of Ni.

***Change in particle morphology and purity of Fe and Ni powder from a mixed metal solution***

Figure 8 shows the morphology of iron seed before and after reduction.



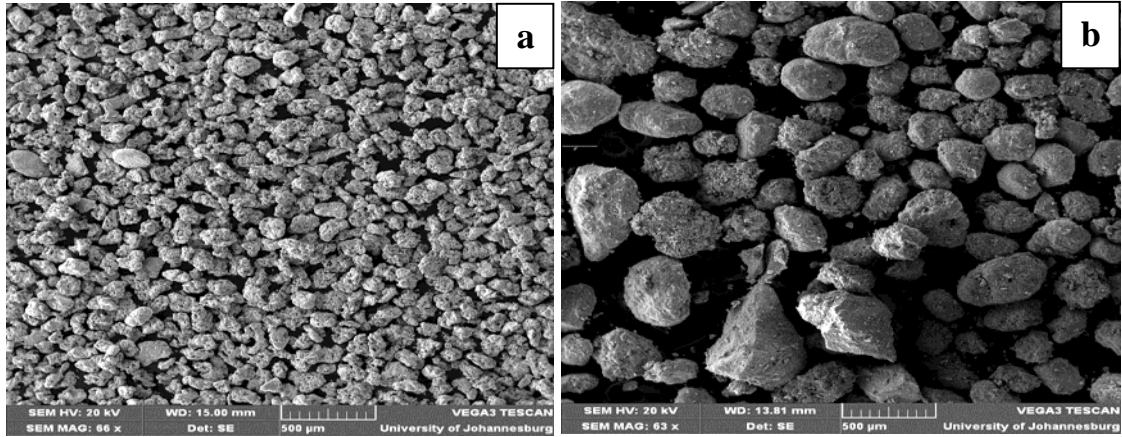


Fig. 8:(a) SEM micrograph of iron seed before reduction and (b) SEM micrograph of iron powder after reduction crystallization

The scanning electron micrographs of the iron seed before and after reduction crystallization are shown in Fig.8 (a) and (b). The particles were smaller before reduction and after the reduction process the particle size increased due to size enlargement. There was also evidence of particle fines and overall the particles were irregular shaped.

The elemental composition of the powder after reduction crystallization using Fe and Ni powder as seeding material is shown in Table 5. The powder purity in terms of the Fe and Ni content decreased for both seeding materials as a result of metal plating. The Fe and Ni content in the seeding material decreased from 96.9% to 74.3% and 99.80% to 93.70% respectively in the powder produced using the mixed Ni-Cu solution. The % Fe and Ni content in both cases decreased because of metal plating, largely of Ni and Cu from solution, incorporation of decomposition products from  $\text{NaBH}_4$  and dissolution of Fe by cementation with Ni for Fe seed.

**Table 5: Powder purity of Fe and Ni powder from the Cu<sup>2+</sup>-Ni<sup>2+</sup>solution**

Elements	Fe	Fe	Ni	Ni
	seed	powder	seed	powder
Na	0.0991	1.18	0.000	1.18
Mg	0.329	0.0921	0.0191	0.0167
Al	0.481	0.171	0.0551	0.128
Si	0.375	0.223	0.0830	0.108
S	0.0871	0.391	0.0130	0.319
Cl	0.0191	0.0192	0.000	0.0212
Fe	96.9	74.3	0.0401	0.0570
Ni	1.24	12.3	99.8	93.7
Cu	0.000	10.9	0.000	4.41
Zn	0.000	0.0484	0.000	0.0271
Ca	0.155	0.151	0.000	0.000

***Evolution of the PSD of powder produced from a mixed metal solution***

Figure 9 shows the evolution of PSD by volume using Fe powder as a seeding material. Pure Fe powder was characterized by uni-modal volume distribution but after reduction the powder was characterized by a bimodal volume distribution as depicted in fig 9(a). The bi-modal distribution is typical of aggregation/agglomeration during particle formation. Fig 9(b) shows that the Fe seed was characterized by a uni-modal mode before reduction and after reduction there was a shift to the left relative to the Fe seed which indicate the generation of smaller sized particles. This trend is similar to that obtained when using Ni as seeding material in a mixed metal solution (Fig. 4).

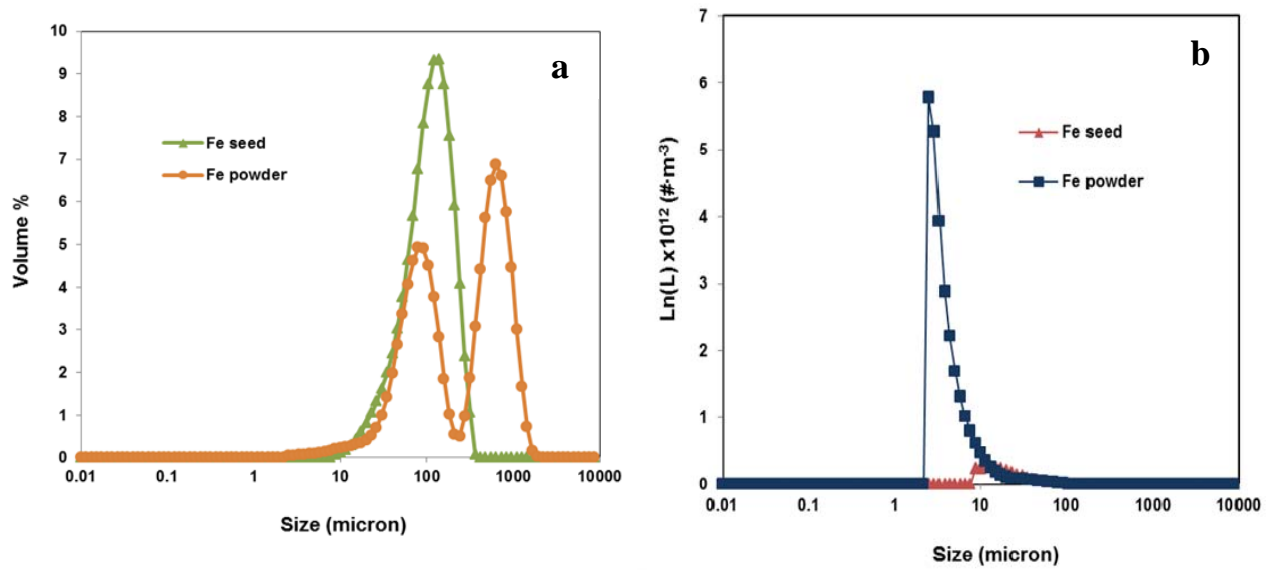


**Fig. 9: (a) Evolution of PSD by volume and (b) Evolution of PSD by number distribution using Fe powder as a seed**

*Moments of the PSD and Crystallization kinetics (mixed metal solution)*

Table 6 shows the particle number and particle external surface area of the seed and the powder produced from a mixed metal solution using a 1:0.1 molar ratio of  $[Ni^{2+}]:[BH_4^-]$  and Fe and Ni powder as seeding material.

**Table 6: Particle number and external surface area of Fe and Ni powder before and after reduction**

	Ni seed	Ni powder	Fe seed	Fe powder
Particle number ( $\# \cdot m^{-3} \times 10^{12}$ )	86.1	325	2.62	5.85
External surface area ( $m^2 \cdot m^{-3} \times 10^3$ )	3.80	2.57	3.03	3.05

There was an increase in particle number and external surface area when Fe powder was used as a seeding material. When Ni was used, there was a decrease in external surface area and an increase in particle number. Both cases are consistent with a process dominated by nucleation and aggregation. The growth, nucleation and aggregation rates calculated using equations 9-12 using Fe and Ni powder as seeding material is shown in Table 7.

**Table 7: Growth, nucleation and aggregation rates using different seeding materials and a mixed metal solution**

Seeding material	$G_0 \times 10^{-8}$ (m.s <sup>-1</sup> )	$B^0 \times 10^{11}$ (no/m <sup>3</sup> s)	$R_a \times 10^{11}$ (no/m <sup>3</sup> s)
Ni	0.457	4.57	1.53
Fe	2.30	0.127	0.0202

The nucleation and aggregation rates were much higher when Ni was used as a seeding material compared to Fe. However, the growth rate was lower for Ni seed as compared to Fe seed, with the later growth rate being comparable to that obtained using Ni seed in a Ni-only solution. The incorporation of Cu in the Ni seeding material results in surface passivation of the Ni particles reducing the catalytic activity and hence the growth rate (Phetla *et al.* 2012). However, its presence in Fe seed did not affect the growth rate, largely because of the ability of Fe to act as a reduction catalyst as also confirmed by previous studies (Phetla *et al.* 2012; Ntuli and Lewis, 2007).

#### ***Statistical comparison of Fe and Ni as seeding materials***

A two sample *t* test assuming unequal variances was used to compute the significance of the difference in % metal removal using Fe and Ni as seeding materials. A *t* value of 0.368 was found for the two tailed test against a *p* critical of 2.776 at 95% confidence interval. Therefore there was no significant difference in the % metal removal of using Fe and Ni as seeding material. Therefore since Fe is cheaper than Ni; Fe is a preferred seeding material.

### ***Determination of precipitation of hydroxides using FTIR***

Figure 10 shows the FTIR spectra of seeding material before and after reduction crystallization.

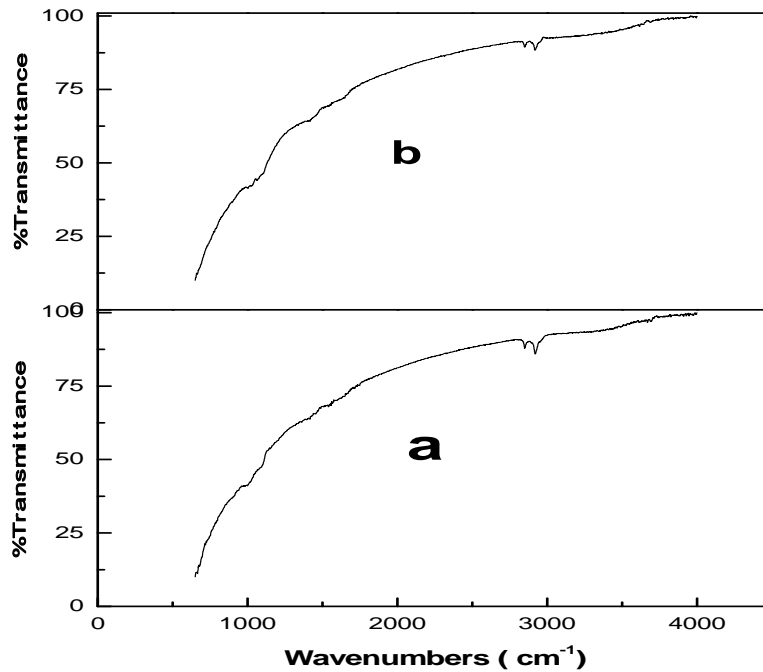


***Fig 10(a) FTIR spectra of Ni powder before reduction crystallization and (b) FTIR spectra of Ni powder after reduction crystallization***

The precipitation of hydroxides was not confirmed by analyzing FTIR spectra as Cu-OH and Ni-OH bands at  $1332\text{cm}^{-1}$  and  $600\text{cm}^{-1}$  respectively are not present in the Ni powder spectrum (Balintova et al, 2012; Boonchom et al, 2008). A qualitative determination for precipitates was performed. When 1M NaOH was added to Ni solution to a pH of 12 pale green precipitate could be seen signifying precipitation of  $\text{Ni}(\text{OH})_2$  whilst the  $\text{Cu}(\text{OH})_2$  formed a blue precipitate which is in agreement with Svehla, 1996. During the reduction crystallization experiment the pale green precipitates were not observed which is further supported by FTIR results (Fig 10).

## CONCLUSION

There was no significant difference in the % removal of Ni and Cu at the molar ratios of  $[\text{Ni}^{2+}]:[\text{BH}_4^-]$  of 1:1, 1:0.25 and 1:0.1. However, the rate of reduction increased with increase in the molar ratio of  $[\text{Ni}^{2+}]:[\text{BH}_4^-]$  from 1:0.1 to 1:1. At  $[\text{Ni}^{2+}]:[\text{BH}_4^-]$  molar of 1:0.1, aggregation and nucleation were the dominant particulate processes, while at molar ratios of 1:0.25 and 1:1, aggregation and growth were the dominant particulate processes. There was no significant difference in the % removal of Ni and Cu using Fe and Ni powder as seeding material. The catalytic activity of Fe powder was not affected by the plating of Cu, while that of Ni decreased with Cu plating. It is thus, recommended that use of Fe powder and  $[\text{Ni}^{2+}]:[\text{BH}_4^-]$  molar ratio of 1:0.1 is adequate for effective removal of Ni and Cu from waste streams.

## Acknowledgment

The authors will like to thank Mining Qualification Authority (MQA) and National Research Foundation (NRF) for their financial assistance.

## References

- Audullah M.M., & Prasad A.G.D., Kinetics and equilibrium studies for adsorption of Cr (VI) from aqueous solution by potato peel waste Research India Publication, (2009) 1-2.
- Bulut Y., & Tez Z., Adsorption studies on ground shells of hazelnut and almond, J. Hazard. Mater. 149 (2007) 35–41.
- Balintova, M., Holub, M., Singovszka, E., Study of Iron, Copper and Zinc Removal from Acidic Solutions by Sorption. Chemical Engineering Transactions, 28 (2012) 1-6.
- Boonchom, B., Youngme, S., Maensiri, S., Danvirutai, C., Nanocrystalline serratbrancaite ( $\text{MnPO}_4 \cdot \text{H}_2\text{O}$ ) prepared by a simple precipitation route at low temperature. Journal of Alloys and Compounds, 454 (2008) 78–82.
- Hasar, H., Adsorption of nickel (II) from aqueous solution onto activated carbon prepared from almond husk, J. Hazard. Mater. 97 (2003) 49–57.
- Hounslow, M.J., Ryall R.L., & Marshall, V.R. A discretized population balance for nucleation, growth, and aggregation. AIChE Journal. 34 (1988) 1821-1832.

Horikawa, and Hirasawa I., "Removal and Recovery of Nickel Ion from Wastewater of Electroless Plating by Reduction crystallization," Korean J. Chem. Eng. 17 (2000) 629-632.

Jianming, L., Dreisinger D.B, and Cooper W.C, "Cobalt precipitation by reduction with sodium borohydride, Hydrometallurgy. 45 (1997) 305-322.

Mallory, G.O., "The fundamental aspects of nickel electroplating," in Electroless Plating: Fundamentals and Applications, G.O. Mallory and J.B. Hadju, Eds. New York: American Electroplaters and Surface Finishers Society. (1990) 4-6.

Moussaouiti, M., Boistelle, R., Bouhaouss A., & Klein J.P., Crystallization of calcium sulphate hemihydrate in concentrated phosphoric acid solutions. Chemical Engineering Journal 68 (1997) 123-130

Naboychenko S.S., "Reduction methods of powder production," in Handbook of non-ferrous metal powders-Technologies and Applications, O.D. Neikov, S.S. Naboychenko & G. Dowson, Eds. Great Britain: Elsevier Ltd.(2009) 171-180.

Ntuli F. & Lewis A.E., The influence of iron on precipitation behaviour of nickel powder, Chemical Engineering Science.62 (2007) 3756-3766.

Phetla T.P, Ntuli F., & Muzenda E. , "Reduction crystallization of Ni, Cu, Fe and Co from a mixed metal effluent, Journal of Industrial and Engineering Chemistry.18 (2012 ), no. 3.

Svehla, G., Vogel's Qualitative Inorganic Analysis, seventh Edition Prentice Hall. (1996).

Tasker, P.A., Tong, C.C., & Westra, A.N., Co-extraction of cations and anions in base metal recovery, Coordination Chemistry Reviews. 251 (2007) 1868–1877.